Instrumented Ankle–Foot Orthosis: Toward a Clinical Assessment Tool for Patient-Specific Optimization of Orthotic Ankle Stiffness

Nicholas B. Bolus, *Student Member, IEEE*, Caitlin N. Teague, *Student Member, IEEE*, Omer T. Inan, *Senior Member, IEEE*, and Géza F. Kogler

***Abstract*—In this paper, we detail the design and operation of the instrumented ankle–foot orthosis (*i*AFO), a clinical assessment tool that can be used to quantify the functional consequences of selectively modifying orthotic ankle joint stiffness, particularly for individuals with locomotor deficits such as foot drop. We discuss the sensing capabilities of the system, which include ankle joint kinematics and kinetics, electromyography, and orthosis interface pressures. We further describe the mechanical design of the device, which allows for user-defined manipulation of orthotic stiffness through an interchangeable extension spring mechanism. Finally, we demonstrate a validation of the *i*AFO's capabilities by presenting results both of benchtop testing and of a preliminary human-subject study. Future work will include in-depth signal analyses of gait parameters and algorithmic development for patient-specific orthosis optimization.**

***Index Terms*—Ankle–foot orthosis (AFO), foot drop, gait analysis, joint impedance, optimized gait, orthosis, orthotic stiffness, wearable.**

I. Introduction

ORTHOSES—WEARABLE devices used to control joint motion and provide corrective support for, or improve the functionality of, impaired limbs/joints—provide a simple, nonoperative, inexpensive, and effective treatment for myriad neuromuscular and musculoskeletal disorders [1], [2]. The most commonly prescribed orthosis is an ankle–foot orthosis (AFO) [3]. In many individuals with a loss of volitional lower-limb motor function, an AFO can provide the necessary stability for standing and walking to enhance functional mobility for the user [4]–[6]. The inability to dorsiflex the foot (i.e., foot drop) is one of the most common lower-limb conditions. Foot drop is associated with peripheral nerve injury, stroke, diabetes, and an array of neurological disorders such as multiple sclerosis and Charcot–Marie–Tooth disease [7]. With reduced ability to lift the foot up toward the shin and thus achieve toe clearance during the swing phase of gait, patients with foot drop often compensate for this deficit, leading to degeneration of normal gait mechanics. The resultant abnormal gait can result in both higher metabolic cost of walking and heightened risk of tripping and falling [8]. Use of lower-limb orthoses to provide stability is common in elderly populations, as the weakening of the ankle dorsiflexors compromises postural control and balance, increasing the risk of injuries caused by falls [9]–[11]. With the rising aging population and incidence of stroke [12], the burden on the orthotics and orthopedics communities will undoubtedly grow heavier, presenting a need for more effective, affordable, and personalized home-use orthoses to improve patient mobility and safety.

AFOs have generally been shown to improve locomotor function (e.g., gait velocity, stride length, walking efficiency, balance) and mitigate injury risk in hemiplegic gait [13]–[18]. However, several studies have shown that, if the devices are not designed or fit properly, such improvements can be relatively insignificant and can in fact cause discomfort and further compromise gait mechanics, perhaps leading to muscle disuse (and eventual atrophy) and reduced patient acceptance of the intervention [19]–[24]. Presently, the methods for determining the proper amount of orthotic resistance are qualitative and subjective. An orthotist typically relies on experiential estimates of the AFO's stiffness by manually deflecting the orthosis, thereby assessing whether the device offers the requisite corrective forces to overcome the motor deficit (e.g., foot drop). The desired treatment outcome of "toe clearance during swing phase" is then clinically confirmed by observational gait analysis. Since the improvements in gait are generally so apparent when adequate resistance to foot drop—and thus swing-phase toe clearance—is achieved, little attention has been devoted to the optimization of orthotic resistance nor to the functional consequences of varying device stiffness—despite studies that have suggested that patient matching of orthotic constraint of motion can significantly influence individual outcomes [24]–[26]. There lacks an objective way of observing and quantifying various parameters of gait in the clinic to identify an optimal set of orthosis

Manuscript received February 3, 2017; revised May 25, 2017, July 25, 2017, and August 18, 2017; accepted September 17, 2017. Date of publication October 10, 2017; date of current version December 13, 2017. Recommended by Technical Editor H. A. Varol. This work was supported in part by the U.S. Army under Grant W81XWH-15-1-0479. The work of N. B. Bolus was supported by the National Science Foundation Graduate Research Fellowship under Grant DGE-1650044. This work expresses the views of the authors only and not necessarily those of the government. *(Corresponding author: Nicholas Bradford Bolus.)*

N. B. Bolus is with the Bioengineering Graduate Program, Georgia Institute of Technology, Atlanta, GA 30332 USA (e-mail: nbolus@gatech.edu).

C. N. Teague and O. T. Inan are with the School of Electrical and Computer Engineering, Georgia Institute of Technology, Atlanta, GA 30332 USA (e-mail: caitlin.n.teague@gmail.com; omer.inan@ece.gatech.edu).

G. F. Kogler is with the School of Biological Sciences, Georgia Institute of Technology, Atlanta, GA 30318 USA (e-mail: geza@gatech.edu).

Color versions of one or more of the figures in this paper are available online at http://ieeexplore.ieee.org.

Digital Object Identifier 10.1109/TMECH.2017.2761746

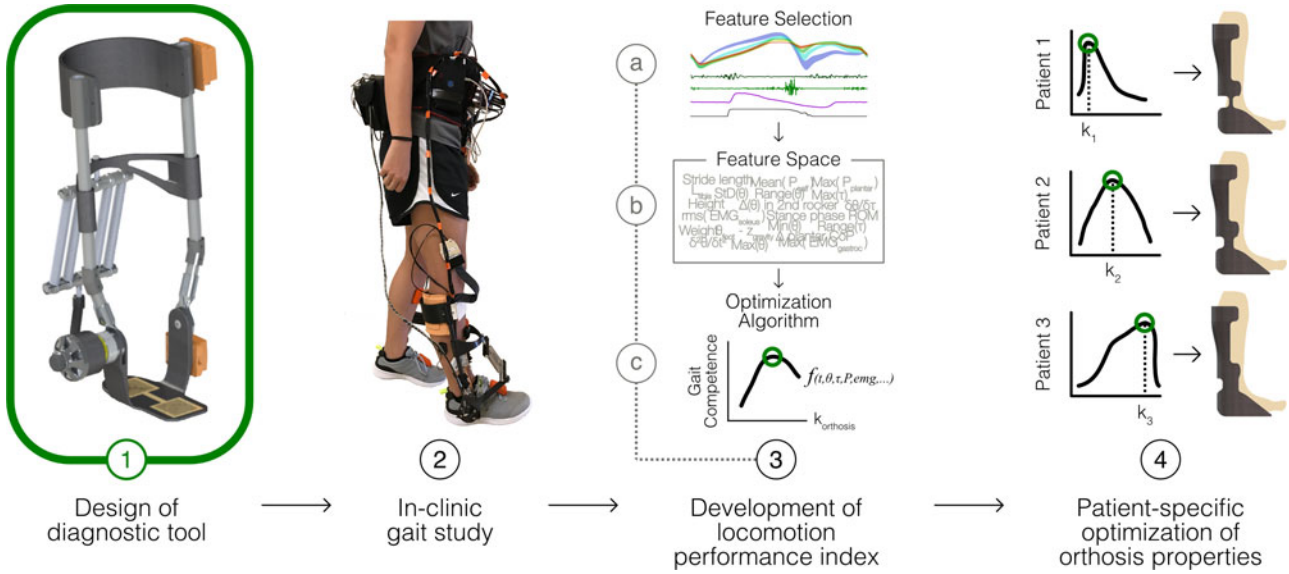

Fig. 1. Broad vision and purpose of the *i*AFO. In this paper, we focus on the design and fabrication step of device development (Phase 1). The *i*AFO is designed to be used as a clinical tool for studying the biomechanics and gait parameters of a pathological gait patient in response to user-defined manipulation of orthotic resistance (Phase 2). Informed by the results of such gait studies, we then intend to develop an index of walking performance and an algorithm for estimating the optimal mechanical properties of an orthosis on a patient-specific basis (Phase 3), which will prime the modeling and fabrication of AFOs customized to each user (Phase 4).

properties for each patient, which may depend on the degree of paresis, paralysis, and spasticity of the lower limb as well as his/her anthropometrics and capacity for recovery. To address this need, we propose the use of an instrumented ankle–foot orthosis (*i*AFO) as a clinical assessment tool to monitor the gait parameters of individuals with disorders affecting movement of the ankle joint.

Numerous efforts have been made to develop powered, active, and adaptive orthoses to assist individuals with movement disorders [27]–[30], employing techniques such as biofeedback via functional electrical stimulation [31], [32], actuated robotic assistance [33]–[37], and variable-impedance joints [38], [39]. While these devices represent major scientific and engineering advances and indeed demonstrate potential as rehabilitation aids, they are currently bulky, complicated, expensive, and unconducive to mass production, making them presently unsuitable for home use. Therefore, in order to maximize clinical impact and most effectively address current patient needs, we elected to focus our work on the domain of passive AFOs.

To that end, the *i*AFO is a passive exoskeletal device comprising an orthotic control feature, which permits a clinician/researcher to modulate ankle joint stiffness with a series of interchangeable extension springs, study a patient's biomechanical response to such a perturbation, and ultimately identify and prescribe an optimal orthosis stiffness on a patient-specific basis (see Fig. 1). Our method for achieving modular orthotic stiffness—i.e., unilaterally applied extension springs—is analogous to the action of a commercial orthosis known as a posterior leaf-spring AFO. This AFO design relies on the elastic deformation of its constituent material (often carbon fiber, metal, or plastic) to control joint motion during walking. Though most of the solid-ankle AFOs constrain joint motion bidirectionally (in contrast to our design, which only imposes rotational resistance in one direction at a time), the *i*AFO preserves the critical functions of a clinically prescribed AFO (i.e., controlling plantarflexion (PF) after initial contact and achieving toe clearance during swing), with comparable mechanical properties to several of the conventional AFOs characterized by Yamamoto *et al.* [40]. Moreover, the benefit of bidirectional orthotic resistance is still debated; some suggest that resistance to PF alone [thus, unimpeded dorsiflexion (DF)] is sufficient or even preferable for improving gait by enabling smooth ankle joint motion during stance phase [41].

The *i*AFO's sensing capabilities allow for monitoring of a patient's sagittal-plane ankle kinematics, kinetics (i.e., applied torque), muscle activity, plantar pressures, and orthotic interface pressures between the device and the user (see Fig. 2). While previous studies using passive AFOs with adjustable stiffness elements have investigated the effect of joint impedance and/or orthosis properties on user joint kinematics [25], [26], [42]–[46], to the best of our knowledge, no prior investigation nor device has employed as comprehensive a sensor suite—in particular, systems to measure orthotic torque and interface pressures directly—to study how gait mechanics change in response to altered joint stiffness. The fact that the *i*AFO is a wearable and portable system (with the exception of the desktop computer used to store and display data, to which the device is cabled) gives it the distinct advantage of being usable in tasks other than normal level walking (to which many gait studies are limited), such as sloped walking, stair walking, and uneven terrain/obstacle evasion tasks (though perhaps difficult, given the device's lack of inversion/eversion rotation), with the potential to be used outside the confines of a gait analysis lab. Wielding this information, a clinician will be able to make informed decisions about how best to modify device geometry, "dose" orthotic stiffness, and even "titrate" this treatment parameter over the course of rehabilitation to optimize locomotor performance, accelerate recovery, minimize atrophy, and improve patient outcomes overall.

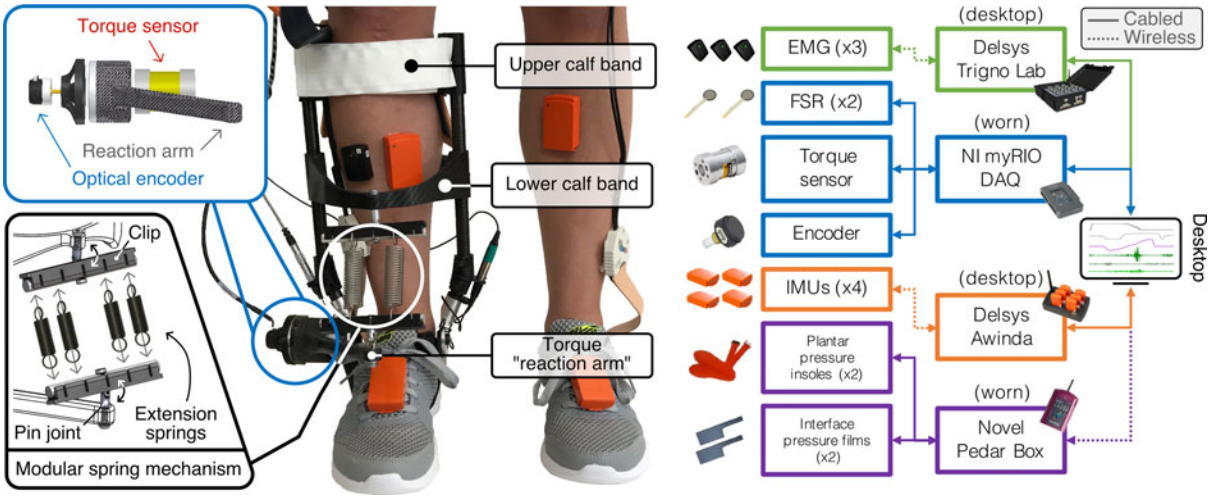

Fig. 2. System-level hardware block diagram. The photo on the left shows a fully instrumented subject, equipped with the *i*AFO with its embedded sensors (torque sensor, optical encoder, and force-sensing resistors) and other standalone sensing systems (EMG, IMU, and pressure-sensitive capacitive films). Sensors that are not visible are the two FSRs and plantar pressure measurement insoles located in the sole of the shoe, as well as the interface pressure sensors located both anteriorly and posteriorly within the calf band. The output of each sensing system is acquired by its corresponding data acquisition unit, synced in time using the myRIO as the master triggering device, and ultimately sent to a desktop computer.

II. Design of the iAFO

A. Custom Chassis Design

The frame of the *i*AFO is comprised entirely of custom-built hardware designed in SolidWorks (Dassault Systèmes, Waltham, MA, USA), with the exception of the tubular uprights, which were purchased from McMaster-Carr Supply (Atlanta, GA, USA). The AFO stirrup and both calf bands—one serving as the upper attachment point for the spring mechanism, the other serving to secure the user's lower leg to the device—are made of a custom carbon composite. Both calf bands are height adjustable, allowing the researcher to modify the device fit based on each user's anatomy, adjust the moment arm of force application to the user's shin/calf in proportion to his/her leg length, accommodate extension springs of different free (i.e., unstretched) lengths, and tune the angle–torque curve to a desired setting (discussed in the Appendix). The torque "reaction arm," formed of the same carbon composite, is fixed to the outer face of the torque sensor and extends medially and anteriorly to the sagittal plane of the user's lower leg. This component allows the torque sensor to directly measure the torque applied by the springs at the ankle joint. The torque reaction arm can be unscrewed and rotated 180°, allowing the springs to be installed either anterior to the shank (thereby resisting PF) or posterior (thus resisting DF). The angled joints that insert into either side of the stirrup are milled out of aluminum 6061-T6, while the custom elbow joints directly superior to them are made of acrylonitrile butadiene styrene (ABS) plastic using a Lulzbot Taz 5 3-D printer (Aleph Objects, Loveland, CO, USA). The device frame alone weighs just 0.6 kg; with sensors embedded, the *i*AFO weighs 0.9 kg; all device peripherals (e.g., data acquisition, interface circuitry, cables), which can be worn in a backpack or (as shown here) in a belt, weigh 2.3 kg.

B. Modular Stiffness Mechanism

The key feature of the *i*AFO is the capacity for user-defined modulation of its torsional stiffness, which is accomplished via interchangeable extension springs. These springs are mounted either anterior or posterior to the shank of the user, enabling one to study the effect of resistance to ankle PF or DF independently (mostly). Springs of various spring rates are mounted in parallel, with each end spaced evenly along an aluminum rod and affixed with a custom clip made out of ABS plastic. The mechanism supports up to five springs installed in parallel, enabling the researcher to study the effects of a wide stiffness gamut. Both ends of the spring attachment mechanism are fixed to the frame of the *i*AFO. When the angle between the device uprights and footplate changes, so too does the distance between spring mounting points, thus deflecting the spring(s). The force developed in the spring(s) causes a resistive torque at the device's joint axis, causing the user to experience a torsional stiffness at the ankle.

C. Sensing and Data Acquisition

To maximize the utility of the *i*AFO as a clinical tool, we equipped it with an extensive sensor suite designed to capture a wide range of clinically relevant biomechanical measures, which are listed in Table I. Signals from the optical encoder, reaction torque sensor, and force-sensitive resistors (FSRs) were acquired directly by a myRIO real-time field-programmable-gate-array-based data acquisition device (National Instruments, Austin, TX, USA), while the remaining sensing systems—inertial measurement units (IMU), plantar/interface pressure sensors, and electromyography (EMG)—required their own proprietary data collection hardware and software. The optical encoder was found to be the optimal angle sensing modality for our application, based on its high resolution, repeatability, and reliability in simulated joint kinematic tests [47]. As they were installed in parallel and not physically integrated into the device, the IMU and EMG systems were considered auxiliary/supportive. As depicted in Fig. 2, in addition to the sensors worn on the ipsilateral limb (the limb with the *i*AFO), two IMUs and one plantar pressure insole were worn on the contralateral limb to investigate potential effects on gait symmetry. (It should

TABLE I
PARAMETERS OF GAIT MEASURED AND SENSORS USED

Parameter	Sensor Type	Manufacturer	Sensor Name	Mfg. Location
Ankle rotation (sagittal plane)	Optical encoder (incremental)	US Digital	S4T	Vancouver, WA, USA
Spatial limb orientation	Inertial measurement unit (IMU)	Xsens	MTw Series	Enschede, The Netherlands
Orthosis torque	Reaction torque, strain gage-based	Futek	TFF350	Irvine, CA, USA
Gait states	Force-sensitive resistor (FSR)	Interlink Elect.	Model 402	Westlake Village, CA, USA
Plantar pressures	Pressure-sensitive capacitive film	Novel	Pedar	Munich, Germany
Interface pressures	Pressure-sensitive capacitive film	Novel	Pliance	Munich, Germany
Muscle activity	Electromyography (EMG)	Delsys	Trigno Lab	Natick, MA, USA

be noted that no data collected from the contralateral limb are reported in this work, as these effects are still being explored. Similarly, IMU data are not reported, as they were considered redundant to kinematic data obtained by the encoder.) Signals from the encoder, torque sensor, and FSRs were recorded by the NI myRIO at a sampling rate of 1 kHz, while plantar- and interface pressures were sampled at 50 Hz, IMU data at 75 Hz, and EMG data at 1926 Hz. All acquired signals were synchronized to facilitate concurrent analysis. The myRIO served as a master triggering device, initiating and terminating acquisition of signals on each sensor system simultaneously. Signals from each sensor subsystem were monitored in real time on a desktop computer. A custom graphical user interface was created in LabView (National Instruments, Austin, TX, USA) to analyze, process, and display signals acquired by the myRIO and to allow for streamlined user control of data collection timing and file management. Custom analog interface circuitry was designed to filter and amplify the output of the strain gage-based reaction torque sensor (low-pass filter with cutoff frequency = 50 Hz, gain = 60.1 dB). In theory, orthotic torque can be calculated given knowledge of the spring mechanics and certain geometrical considerations (see the Appendix), but given uncertainties in real-world implementation (e.g., friction, nonlinear spring force, and fatigue), we considered direct measurement of torque necessary to obtain the most accurate information possible. All circuitry and peripheral devices (e.g., myRIO, synchronization boxes, pressure sensor DAQ, and battery power) are worn either at the waist or housed in a backpack.

D. System Specifications

A summary of the key features of the *i*AFO system can be found in Table II, including metrics of device wearability and functionality as well as a few important sensor specifications. Certain parameters such as orthotic torque capacity and range of linear torque application are setup-dependent (i.e., the former depends on the available range of spring stiffness values, while the latter depends on the calf-band height setting, as discussed previously). In all, these attributes suggest a highly modular, versatile, and effective tool for selectively modifying orthotic stiffness and for thorough monitoring of an expansive set of gait parameters.

TABLE II
IAFO SYSTEM SPECIFICATIONS

Parameter	Value
Size and Wearability	
Weight	0.9 kg (fully instrumented)
Overall dimensions	40 × 23.5 × 21 cm
Calf-band height adjustability range	10–32.5-cm proximal ankle
Shoe size accommodation	U.S. size 7–13
Sensor Specifications	
Torque measurement range	±56.5 N·m (500 in·lb)
Angle measurement resolution	0.25°
Sampling Rates	1 kHz (joint angle, torque, FSRs), 50 Hz (interface/plantar pressures), 1926 Hz (EMG), 75 Hz (IMU)
Functionality	
Parameters monitored	Ankle joint angle, orthotic torque, plantar/interface pressures, EMG, lower-limb orientation, gait states
Orthotic resistance modes	PFR, DFR (independently)
Orthotic ankle torque capacity[a]	±15 N·m
Range of linear torque application[b]	–15° to 10°
Angle measurement plane	Leg sagittal

[a]Dependent on springs applied; rated here for stiffest available springs at peak DF/PF angle achieved; likely higher for greater spring rates.
[b]Dependent on L0, preload, and attachment height setting of spring(s) (see the Appendix).

III. EXPERIMENTS AND RESULTS

A. Benchtop Testing

1) Benchtop Experimental Setup: To characterize the performance of the *i*AFO and demonstrate how it resists ankle rotation, we performed benchtop tests and compared the results to those of an actual gait study. In particular, we were interested in the device's angle–torque relationship in the sagittal plane of the foot/ankle. In the benchtop experiments, the device's footplate was clamped to a tabletop and its upper frame was rotated back and forth by hand approximately 15° in both PF and DF. (NB: This paper adheres to classical ankle measurement conventions—i.e., "0°," or neutral, is defined as when the shank is perpendicular to the foot, PF is defined as the range of negative angles, and DF is defined as the range of positive angles.) Two different stiffness conditions—defined simply as the sum of spring rates, as springs were applied in parallel—were applied: 350 and 1540 N/m, as these two values represented the lower and upper ends of orthotic restraint investigated in human subject trials. The device angle and torque were recorded by the optical encoder and reaction torque sensors, respectively, and the data were acquired by the NI myRIO data acquisition device. The torque versus angle relationship obtained from the benchtop tests was then compared to that of the human subject experiment (detailed further below). Additionally, we developed a mathematical model to describe how the device's geometric parameters inform the shape of the angle–torque curve in the angle range of interest and thus how, for a given stiffness con-

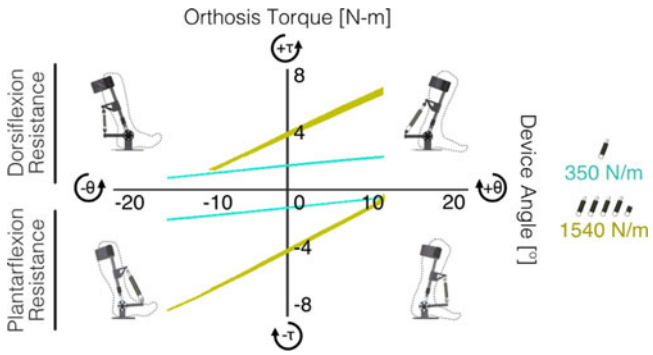

Fig. 3. Benchtop testing results: orthotic torque versus angle relationship in both resistance modes for two stiffness conditions. The two curves above the *x*-axis were generated with the device in its DFR mode (i.e., extension springs mounted posterior to the calf), while the curves below the *y*-axis correspond to the device in its PFR mode. In the angle regime of interest (–15° to 15°), the device applies torque in a linear fashion and does so nearly equivalently in both resistance modes.

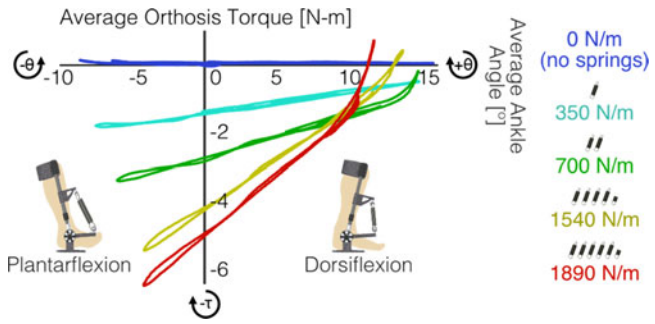

Fig. 4. Orthotic torque versus ankle angle relationship in PFR gait study. Five stiffness conditions were considered, and torque was applied to the user linearly, just as in the benchtop experiments. Some amount of nonlinearity and hysteresis were observed, though these were relatively negligible across most of the ankle range of motion. The curves above represent the ensemble average of individual torque versus angle curves across approximately 50 steps.

dition, this relationship can be "tuned" by a simple adjustment of the calf-band height setting. This information can be found in the Appendix.

2) (Device-Only) Torque Versus Angle Relationship: The results of benchtop testing (see Fig. 3) demonstrate that, with either plantarflexion resistance (PFR) or dorsiflexion resistance (DFR), the *i*AFO appears to apply torque linearly across the ankle angle range, comparable to the linear-elastic region of a material's torsional stress–strain curve. The curves of each stiffness condition (i.e., each pair of same-color curves) appear to have similar slopes in both resistance modes (for the "350 N/m" setting: 0.056 N·m/° in DFR and 0.058 N·m/° in PFR, 4.4% difference; for the "1540 N/m" setting: 0.27 N·m/° in DFR and 0.30 Nm/° in PFR, 9.7% difference), suggesting the *i*AFO operates similarly in DFR and PFR.

B. Human Subject Pilot Study

1) Pilot Study Protocol: To demonstrate the *i*AFO's potential for use in clinical gait study applications, we fit the device to the right leg of a healthy male subject (age: 23, weight: 68 kg) and performed normal, level walking trials at a variety of orthotic stiffness settings. Locomotion took place on a treadmill at a constant speed of 1.0 m/s. Five stiffness conditions were investigated, including 0 (i.e., unloaded/no springs), 350, 700, 1540, and 1890 N/m. For this range of stiffness values, a maximum of 7 N·m of DF-assist torque was reached at 10° of PF, consistent with the lower end of the range that Yamamoto *et al.* suggested is necessary for individuals with pathological gait [42] and consistent with the torques that they found most solid-ankle, plastic AFOs produced [40]. We believe this to be a sensible range for healthy subjects, though the modularity of our stiffness control mechanism allows us to adjust the maximum stiffness, should it be required for users with hemiplegic gait. Data were recorded for 100 s per trial. The subject was allowed to walk in the device for an extended period of time (∼5–10 min) before collecting data to minimize the possible confounding effect of motor adaptation on experimental results. Orthotic stiffness challenges were administered randomly, and each condition was repeated three times over the course of data collection to establish the consistency of results. PFR and DFR modes were evaluated independently, though only the results of PFR experiments are presented below, as we believe they more validly represent the effect (and purpose) of an AFO designed for an individual with foot drop, for whom assistance in DF (i.e., PFR) is critical.

2) (Device+User) Torque Versus Angle Relationship: The torque–angle curves obtained during a human subject experiment (see Fig. 4) were consistently quite linear. The curves shown in Fig. 4 resulted from an experiment performed solely in the device's PFR mode, and they represent the relationship between the device's angle and torque curves, averaged over the course of a full data collection trial (∼50 gait cycles). The torque versus angle curves for the 350 and 1540 N/m stiffness conditions have slopes nearly equivalent to those obtained in benchtop experiments (for the "350 N/m" setting: 0.72% difference; for the "1540 N/m" setting: 2.9% difference). A small amount of hysteresis—suggesting the orthosis applied torque differently in loading versus unloading at moderately high-frequency cycling—is present in the extreme angles of the three highest stiffness conditions, perhaps due to internal friction of the springs or the viscoelastic influence of the leg's soft tissues.

One noteworthy feature of the data from the human subject gait study is the apparent nonlinearity of the angle–torque curve at the end range of DF. This aberration occurs when the extension springs, in their fully compressed state, press into the torque reaction arm when the angle between the tibia and the foot is sufficiently acute. This action causes the torque sensor to register values in the opposite direction of desired torque application. This behavior speaks to an inherent limitation in the device's ability to apply end-range orthotic resistance. To minimize this nonlinearity in the PFR mode, we ensured that the springs remained minimally extended at the highest expected angle of DF (∼20°) by adjusting the height setting of the spring attachment mechanism. The tradeoff in doing so is the imperfect separation of orthotic resistance into either DFR or PFR and, effectively, an adjustment of the neutral angle of the device (i.e., the angle at which the device applies zero torque). We used our geometric model of the *i*AFO (see the Appendix) as a guide to balance the tradeoff between full directional separation of orthotic resistance and end-range torque–angle curve linearity. Indeed, this ability to select the neutral angle of the device may, in some cases, be considered a design advantage, as it has been shown

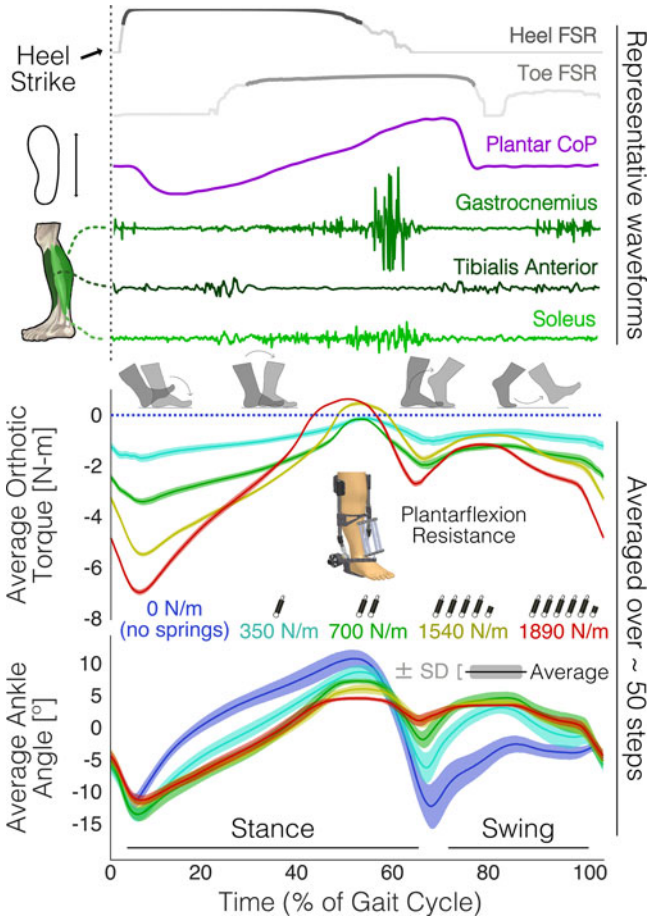

Fig. 5. Results of PFR experiment ($n = 1$). All waveforms are synchronized in time across a single gait cycle. The top six waveforms are simply representative of sensor outputs for a single step, and the bottom two plots are comprised (respectively) of orthotic torque and ankle angle waveforms averaged across approximately 50 steps, plotted against the percentage of one gait cycle. A key finding of this experiment, illustrated in the bottom plot, is a marked attenuation of ankle excursion in both the terminal stance and swing phases of gait with increasing orthotic resistance.

that an AFO's neutral (or "initial") angle can greatly impact a user's gait kinematics and mobility [26], [48].

3) Proof-of-Concept Gait Parameters: Fig. 5 illustrates several signals of interest that the *i*AFO is able to record on a continuous step-to-step basis. All waveforms depict signal behavior across the gait cycle, beginning with initial contact ("heel-strike") and ending with terminal swing. The top six waveforms (FSR, pressure measurement insole, and EMG) are simply representative samples of data isolated for a single step under a single stiffness condition and are left unitless, as (in this discussion) their shapes are more meaningful than their numeric values, and they serve mainly as a demonstration of the sensing capabilities of the system. IMU data are not reported here, as they were considered redundant to the kinematic data obtained by the optical encoder; however, the use of IMUs for discerning deviations between device angle and the user's anatomical joint angle is still being explored. Furthermore, as this work is still preliminary, only data from the sensors embedded in the device (encoder, torque sensor) are reported across all stiffness conditions; trends in other gait parameters will be investigated in future work.

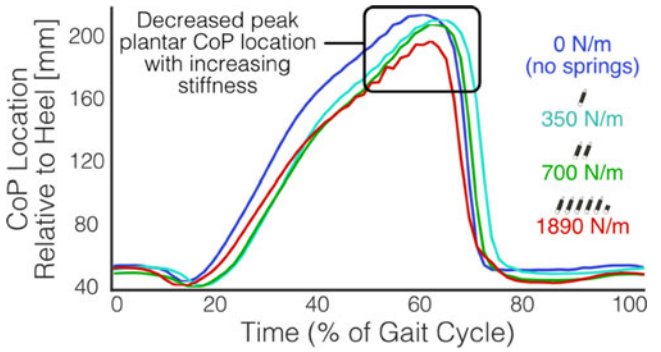

Fig. 6. Average plantar CoP location changes with increasing orthotic resistance. Here, CoP location is defined as the lengthwise distance along the right foot beginning at the back of the heel, measured in millimeters. Peak CoP location decreased progressively from 216 to 213.5 to 210.1 and finally to 202.3 mm for each increasing stiffness challenge, suggesting a diminished ability to transfer plantar forces toward the forefoot, likely resulting in a decrease in the anatomical torque produced by the individual at the ankle joint.

a) Plantar force/pressure: The "Heel FSR" and "Toe FSR" signals are used simply to delineate states of gait and to serve as a timing reference for windowing the continuous data into individual steps for subsequent averaging and analysis. The "plantar center of pressure" (CoP) waveform was obtained from the Novel Pedar plantar pressure measurement system. The curve corresponds to the location of the plantar CoP along the lengthwise axis of the subject's right foot over the course of a gait cycle: beginning at a neutral location at the very beginning of stance phase, moving closer toward the heel during the loading response phase, and traveling distally along the foot toward the metatarsals at push-off, before finally returning to a neutral position during swing phase. A comparison of the average CoP waveforms across stiffness conditions (shown in Fig. 6) reveals a trend toward decreasing peak distance of CoP along the length of the foot with increasing orthotic resistance.

This finding suggests that, with a stiffer DF-assistive AFO, a person may not be able to apply plantar forces as far forward during late-stance and thus reduce his/her capacity to push off effectively, perhaps reducing stride length and gait efficiency.

b) Muscle activity: The three EMG waveforms shown in green in Fig. 5 illustrate, respectively, the activity of the gastrocnemius, tibialis anterior, and soleus muscles during a single gait cycle, and the recorded waveforms align logically with each one's anatomical function–that is, the plantarflexors (gastrocnemius and soleus) demonstrate increased activity during stance phase and push-off, while the tibialis anterior (an ankle dorsiflexor) is more active during loading response and swing phase [49].

While not especially revelatory in this preliminary healthy subject experiment, we anticipate EMG data will be particularly useful in discerning the timing of muscle activation during each phase of gait and determining whether, or how, this timing is disrupted in hemiplegic gait patients as a result of the modulation of orthotic constraint. But for the purposes of this work, the waveforms simply demonstrate our system's ability to monitor muscle activity concurrently with various other gait parameters of clinical interest.

c) Ankle angle and orthotic torque changes across five stiffness conditions: The bottom two plots of Fig. 5

represent the key findings of our preliminary pilot study. Each plot is comprised of several ensemble-averaged waveforms (±SD) of orthotic torque (top) and ankle joint angle (bottom) for each of the stiffness conditions listed previously. The average orthotic torque plot, illustrating the change in torque applied by the *i*AFO to the user, shows a distinct and proportional change in the amount of rotational resistance for each successive applied stiffness. The errant behavior of the highest two stiffness conditions at around 40–50% of the gait cycle where the torques appear to change sign (i.e., from counter-clockwise to clockwise, or PFR to DFR) is a product of the same phenomenon explained above (i.e., the unstretched springs bearing down upon the torque reaction arm during pronounced DF). Nonetheless, the graph clearly demonstrates an increase in torque magnitude with increasing stiffness (as expected) and illustrates the high repeatability of the signal, as evidenced by the low standard deviation error bars on each average waveform. The bottom plot illustrates the marked changes in ankle range of motion resulting from modulation of orthotic stiffness. The most obvious stratifications occur toward the end of stance and beginning of swing, where an increased resistance to PF results in a substantial reduction in ankle joint excursion during the second rocker (i.e., when the tibia processes over the ankle)—seen here as a reduction in the peak DF angle at the end of stance phase—as well as a significant attenuation of ankle excursion during "push-off," in which the foot rapidly plantarflexes to propel the person forward. A significant decrease in full ankle range of motion (i.e., the peak-to-peak amplitude of each average angle waveform) is also apparent with increasing stiffness challenge.

One possible explanation for the reduction in stance-phase DF is that the subject is attempting to maintain a symmetrical gait: the springs resist ankle PF during the loading response phase, thus prolonging that motion; in order to compensate, the subject may then abbreviate the following phase(s), shortening the step and thus not advancing the limb as far forward. Or perhaps it is a product of the subject simply fighting against any perceived perturbation, either resistive or assistive—though a more detailed biomechanical analysis is needed to make a definitive claim.

IV. Discussion

A. Clinical Relevance and Potential Applications

As mentioned previously, the traditional methods for evaluating AFO-assisted gait are often subjective and imprecise. If deployed in a clinical setting, the *i*AFO could provide practitioners with a wealth of potentially useful information for prescribing an orthosis with optimal stiffness. With the sensors proposed, the system could report—in real time and with high resolution and temporal detail—gait parameters such as ankle joint range of motion (both overall and in each discrete phase of gait), peak torque applied by the device, biomechanical "power" lost to the device across a gait cycle, time spent in single-limb support on the affected limb, changes to gait symmetry, peak impulse (force-time integral) applied at the device-to-user interface (perhaps a measure of discomfort or how much energy is lost to the device), training/motor-learning effects over time, and ankle angle and amount of "shock" (peak acceleration) at initial contact (indicating how effectively momentum is preserved step-to-step). Information of this nature would be impossible to attain through observational gait analysis alone, and much of it would be unattainable even given state-of-the-art motion capture setups.

Coupling these sensory capabilities with the *i*AFO's modular stiffness feature will allow researchers to understand the implications of orthotic stiffness on a deeper level than previously possible. For instance, studies employing the *i*AFO may reveal—in great detail and on a case-by-case basis—correlations between AFO stiffness and stance-phase stability, mitigation of toe drag, reduction in steppage gait, improvement in stride length symmetry, etc. With this greater depth of understanding, a clinician could, for example, target a higher DF stiffness to prioritize stance stability for an elderly patient whose critical need is the prevention of falls. Likewise, a patient with severe PF contracture could be prescribed an AFO tuned to a higher PF stiffness to correct for this malady.

Data collected from *i*AFO-enhanced gait studies would supplement more traditional clinical criteria such as gait velocity and patients' subjective assessment of comfort to form a comprehensive, evidenced-based AFO stiffness prescription pathway. Furthermore, these gait studies could be performed iteratively along the course of rehabilitation, allowing for adjustments to a patient's "stiffness regimen" over time as results dictate.

B. Limitations

While the *i*AFO boasts many positive design characteristics (e.g., robust construction, high modularity, and extensive sensing capabilities), it also has a few limitations. For instance, the method of applying orthotic restraint (via unilaterally applied extension springs), though simple and user-friendly, is not an ideal way to simulate the mechanical characteristics of a true solid-ankle AFO commonly used in clinical practice. The reasons for this shortcoming have been discussed previously, but as stated before, we found that our device applied orthotic restraint in a way which corresponds favorably to the results found by Yamamoto *et al.* for several commercial AFOs [40]. In the future, we plan to refine our design to incorporate springlike elements that can provide orthotic resistance in both directions simultaneously and can be adjusted continuously, perhaps using compression springs, series-elastic actuators to serve as "tunable" springs, a disengaging clutch mechanism such as the one used by Collins *et al.* [50], or a continuous "mechanical impedance adjuster" such as developed by Morita and Sugano [51]. Additionally, our device requires the use of a set of shoes modified to accommodate its dimensions, meaning it cannot simply be slipped into any patient's preferred footwear. This is done out of necessity to ensure a proper seating of the device in the shoe and to minimize the effect of variations in shoe composition, shape, and overall design on between-subject results. Finally, our device, as with the majority of articulated AFOs, limits ankle joint action to rotation in the sagittal plane, impeding compound joint motions that involve foot inversion and eversion.

V. Conclusion

The prevalence of lower-limb motor impairments and the relative lack of quantitative outcome measures for therapeutic solutions presents both a gulf in the clinical approach to treatment as well as a compelling opportunity for the development and implementation of devices designed to diagnose and quantify specific deficits, assess the efficacy of treatment and the pace of recovery, and ultimately inform patient-specific approaches to

treatment optimization. We believe that our device, the *i*AFO, represents a significant advancement toward objective assessment and optimization of ankle–foot orthoses for the treatment of foot drop and potentially other motor deficits impacting the lower limb. With its extensive sensor suite, robust construction, and capacity for user-defined stiffness modulation, we believe it is a clinical tool well suited to the diagnosis and study of foot drop in particular, as well as a scientific tool for studying how manipulating ankle joint stiffness affects locomotor function. Our validation tests demonstrate that the *i*AFO is capable of both applying orthotic resistance and monitoring an extensive set of relevant physiological parameters in a repeatable and reliable manner. The results of a pilot study using the *i*AFO, though preliminary, are striking and suggest a noteworthy change in a healthy person's ankle joint kinematics in response to perturbations of the ankle joint, though a more thorough analysis of other signals (e.g., EMG and interface pressures) and a larger and more anatomically diverse subject population is required to make any definitive claims. Nonetheless, the quality and comprehensiveness of the data collected present a rich opportunity for further robust data analysis and algorithmic development, particularly in forthcoming studies on populations with gait abnormalities such as foot drop. Furthermore, these results serve as a proof of concept for our device and highlight its capabilities in gait studies of this sort, making us optimistic for future investigations, applications, and developments of the *i*AFO.

APPENDIX

To better our understanding of the mechanical behavior of the *i*AFO, we endeavored to supplement the insights gained from benchtop testing with the development of a simplified geometric model whereby, given some input parameters (e.g., calf-band height and applied stiffness condition), we could predict the angle–torque curve that the device would exhibit within the range of motion of the user's ankle joint. In doing so, we hoped to mitigate issues of end-range torque nonlinearity and incomplete separation of torque application into either rotation direction (DF or PF) by selecting an appropriate calf-band height setting. The "calf band" referenced here is the lower one on which the spring attachment mechanism is mounted, not the one that bears user force input; therefore, we are effectively describing changes in the mounting position of the spring. Fig. 7 illustrates the geometric parameters used in the following equations that are used to construct the mathematical model of the torque versus angle relationship:

$$\vec{r}_{\mathrm{mount,high}} = f\left(\theta_{\mathrm{ankle}}, z_{\mathrm{calfband}}\right) \tag{1}$$

$$\vec{r}_{\mathrm{spring}} = \vec{r}_{\mathrm{mount,low}} - \vec{r}_{\mathrm{mount,high}} \tag{2}$$

$$\tau = \vec{r}_{\mathrm{mount,low}} \times \left\{ k_{\mathrm{spring}} \left[\vec{r}_{\mathrm{spring}} - \frac{\vec{r}_{\mathrm{spring}}}{\|\vec{r}_{\mathrm{spring}}\|} L_0 \right] \right\}. \tag{3}$$

Equation (1) suggests that $\vec{r}_{\mathrm{mount,high}}$, the vector from the center of rotation at the ankle joint to the upper attachment point of the spring(s), is simply a (trigonometric) function of z_{calfband}, which is the adjustable calf-band height setting, and θ_{ankle}, which is the rotation of the user's ankle joint, measured clockwise from the positive vertical axis. Equation (2) defines $\vec{r}_{\mathrm{spring}}$ as the vector difference between $\vec{r}_{\mathrm{mount,high}}$ and $\vec{r}_{\mathrm{mount,low}}$, which is the vector from the center of the ankle joint to the lower attachment point of the spring mechanism. The final calculation relating torque and ankle angle is shown in (3), where τ is the calculated orthotic torque applied to the user, k_{spring} is the stiffness condition, and L_0 is the free length of the spring(s) used. The term within the curly braces represents the force developed in the extension spring(s) due to lengthening, calculated using Hooke's Law. Since the springs are nonideal and are manufactured with a preload, k_{spring} was determined experimentally on a benchtop setup for a range of spring deflections in order to improve the accuracy of the model.

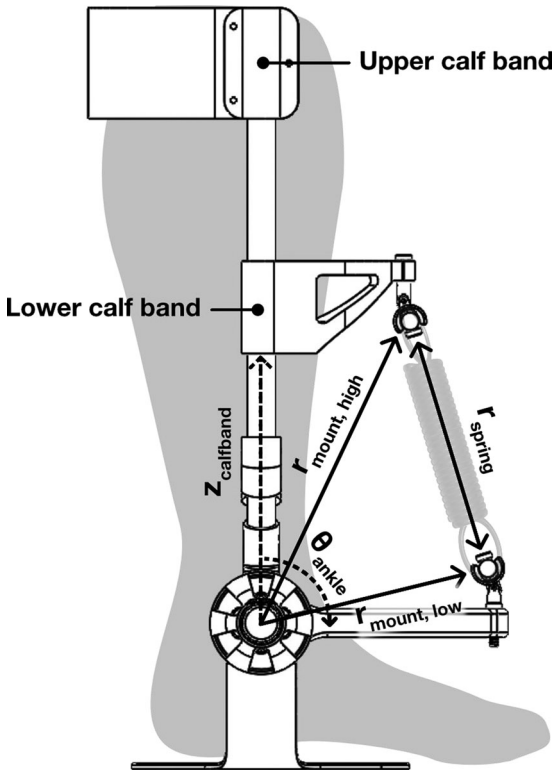

Fig. 7. Geometric model of the *i*AFO, lateral view. As shown, the device is in its PFR mode. Each of the vectors defined here is used to predict the geometric relationship between ankle joint excursion and spring deflection and thus the amount of torque applied by the device, a relationship which defines the degree of orthotic constraint.

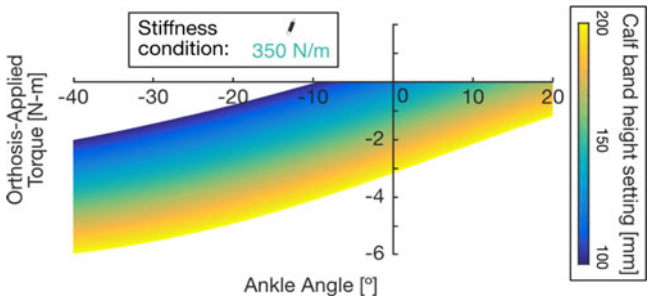

Fig. 8. Example of model torque versus angle output for a range of calf-band height settings (resistance mode: PFR, stiffness condition: 350 N/m). Each isochromatic curve corresponds to a specific height setting. For our tests, we chose a height setting of 160 mm, which gave us a good balance for isolating resistance into PF and mitigating nonlinearity at high angles of DF. Only torques in the PFR regime are shown.

Fig. 8 shows the result of these calculations for a range of calf-band height settings (from 100 to 200 mm, referenced from the ankle joint center) and across a range of ankle angles, with the device in its PFR mode and for the 350 N/m stiffness condition. The model is moderately accurate in predicting true device behavior in the range of PFR torque (i.e., the negative y-axis, in which the springs are extended). The model predictions in the positive torque regime are excluded from the figure, as they are not a faithful representation of the device's behavior in end-range DF. The model is useful primarily as a means to understand (in general) how the torque–angle relationship can be modulated, particularly around $\theta_{\text{ankle}} = 0°$, by changing the height setting of the spring attachment, which can be gleaned from the plot.

REFERENCES

[1] J. D. Hsu *et al.*, *AAOS Atlas of Orthoses and Assistive Devices*. Amsterdam, The Netherlands: Elsevier, 2008.

[2] S. Hoppenfeld and V. L. Murthy, *Treatment and Rehabilitation of Fractures*. Philadelphia, PA, USA: Lippincott Williams & Wilkins, 2000.

[3] S. Whiteside *et al.*, *Practice Analysis of Certified Practitioners in the Disciplines of Orthotics and Prosthetics*. Alexandria, VA, USA: American Board for Certification in Orthotics, Prosthetics & Pedorthics, 2007.

[4] E. Cakar *et al.*, "The ankle-foot orthosis improves balance and reduces fall risk of chronic spastic hemiparetic patients," *Eur. J. Phys. Rehabil. Med.*, vol. 46, no. 3, pp. 363–368, 2010.

[5] R.-Y. Wang *et al.*, "Gait and balance performance improvements attributable to ankle–foot orthosis in subjects with hemiparesis," *Amer. J. Phys. Med. Rehabil.*, vol. 86, no. 7, pp. 556–562, 2007.

[6] B. M. Rogozinski *et al.*, "The efficacy of the floor-reaction ankle-foot orthosis in children with cerebral palsy," *J. Bone Joint Surg. Amer.*, vol. 91, no. 10, pp. 2440–2447, 2009.

[7] C. Sackley *et al.*, "Rehabilitation interventions for foot drop in neuromuscular disease," *Cochrane Database Syst. Rev.*, vol. 3, 2009, Art. no. CD003908.

[8] J. D. Stewart, "Foot drop: Where, why and what to do?" *Practical Neurol.*, vol. 8, no. 3, pp. 158–169, 2008.

[9] J. L. O'Loughlin *et al.*, "Incidence of and risk factors for falls and injurious falls among the community-dwelling elderly," *Amer. J. Epidemiol.*, vol. 137, no. 3, pp. 342–354, 1993.

[10] B. H. Alexander *et al.*, "The cost and frequency of hospitalization for fall-related injuries in older adults," *Amer. J. Public Health*, vol. 82, no. 7, pp. 1020–1023, 1992.

[11] M. E. Daubney and E. G. Culham, "Lower-extremity muscle force and balance performance in adults aged 65 years and older," *Phys. Therapy*, vol. 79, no. 12, p. 1177, 1999.

[12] V. L. Roger *et al.*, "Heart disease and stroke statistics—2011 update a report from the American Heart Association," *Circulation*, vol. 123, no. 4, pp. e18–e209, 2011.

[13] J. Leung and A. Moseley, "Impact of ankle-foot orthoses on gait and leg muscle activity in adults with hemiplegia: Systematic literature review," *Physiotherapy*, vol. 89, no. 1, pp. 39–55, 2003.

[14] L. A. B. Ferreira *et al.*, "Effect of ankle-foot orthosis on gait velocity and cadence of stroke patients: A systematic review," *J. Phys. Therapy Sci.*, vol. 25, no. 11, pp. 1503–1508, 2013.

[15] H. Abe *et al.*, "Improving gait stability in stroke hemiplegic patients with a plastic ankle-foot orthosis," *Tohoku J. Exp. Med.*, vol. 218, no. 3, pp. 193–199, 2009.

[16] H. Gök *et al.*, "Effects of ankle-foot orthoses on hemiparetic gait," *Clinical Rehabil.*, vol. 17, no. 2, pp. 137–139, 2003.

[17] D. Bregman *et al.*, "Spring-like ankle foot orthoses reduce the energy cost of walking by taking over ankle work," *Gait Posture*, vol. 35, no. 1, pp. 148–153, 2012.

[18] N. G. Harper *et al.*, "The influence of ankle-foot orthosis stiffness on walking performance in individuals with lower-limb impairments," *Clinical Biomech.*, vol. 29, no. 8, pp. 877–884, 2014.

[19] N. Eddison *et al.*, "Ankle foot orthosis–footwear combination tuning: An investigation into common clinical practice in the United Kingdom," *Prosthetics Orthotics Int.*, vol. 39, pp. 126–133, 2014.

[20] J. De Vries, "Evaluation of lower leg orthosis use following cerebrovascular accident," *Int. J. Rehabil. Res.*, vol. 14, no. 3, pp. 239–243, 1991.

[21] B. Meadows, "Tuning of rigid ankle-foot orthoses is essential," *Prosthetics Orthotics Int.*, vol. 38, no. 1, pp. 83–83, 2014.

[22] A. J. Ries *et al.*, "A data driven model for optimal orthosis selection in children with cerebral palsy," *Gait Posture*, vol. 40, no. 4, pp. 539–544, 2014.

[23] J. F. Geboers *et al.*, "Immediate and long-term effects of ankle-foot orthosis on muscle activity during walking: A randomized study of patients with unilateral foot drop," *Arch. Phys. Med. Rehabil.*, vol. 83, no. 2, pp. 240–245, 2002.

[24] C. A. Crabtree and J. S. Higginson, "Modeling neuromuscular effects of ankle foot orthoses (AFOs) in computer simulations of gait," *Gait Posture*, vol. 29, no. 1, pp. 65–70, 2009.

[25] T. Sumiya *et al.*, "Stiffness control in posterior-type plastic ankle-foot orthoses: effect of ankle trimline Part 2: Orthosis characteristics and orthosis/patient matching," *Prosthetics Orthotics Int.*, vol. 20, no. 2, pp. 132–137, 1996.

[26] S. Yamamoto *et al.*, "Quantification of the effect of the mechanical property of ankle-foot orthoses on hemiplegic gait," *Gait Posture*, vol. 1, no. 1, pp. 27–34, 1993.

[27] A. J. Young and D. P. Ferris, "State-of-the-art and future directions for robotic lower limb exoskeletons," *IEEE Trans. Neural Syst. Rehabil. Eng.*, vol. 25, no. 2, pp. 171–182, Feb. 2017.

[28] T. Yan *et al.*, "Review of assistive strategies in powered lower-limb orthoses and exoskeletons," *Robot. Auton. Syst.*, vol. 64, pp. 120–136, 2015.

[29] K. A. Shorter *et al.*, "Technologies for powered ankle-foot orthotic systems: Possibilities and challenges," *IEEE/ASME Trans. Mechatronics*, vol. 18, no. 1, pp. 337–347, Feb. 2013.

[30] A. Pennycott *et al.*, "Towards more effective robotic gait training for stroke rehabilitation: A review," *J. Neuroeng. Rehabil.*, vol. 9, no. 1, 2012, Art. no. 65.

[31] M. Goldfarb and W. K. Durfee, "Design of a controlled-brake orthosis for FES-aided gait," *IEEE Trans. Rehabil. Eng.*, vol. 4, no. 1, pp. 13–24, Mar. 1996.

[32] D. P. Ferris *et al.*, "An improved powered ankle–foot orthosis using proportional myoelectric control," *Gait Posture*, vol. 23, no. 4, pp. 425–428, 2006.

[33] K. A. Shorter *et al.*, "A portable powered ankle-foot orthosis for rehabilitation," *J. Rehabil. Res. Develop.*, vol. 48, no. 4, pp. 459–472, 2011.

[34] A. Roy *et al.*, "Robot-aided neurorehabilitation: A novel robot for ankle rehabilitation," *IEEE Trans. Robot.*, vol. 25, no. 3, pp. 569–582, Jun. 2009.

[35] M. Moltedo *et al.*, "Mechanical design of a lightweight compliant and adaptable active ankle foot orthosis," in *Proc. 6th IEEE Int. Conf. Biomed. Robot. Biomechatronics*, 2016, pp. 1224–1229.

[36] N. Vitiello *et al.*, "Functional design of a powered elbow orthosis towards its clinical employment," *IEEE/ASME Trans. Mechatronics*, vol. 21, no. 4, pp. 1880–1891, Aug. 2016.

[37] D. P. Ferris *et al.*, "An ankle-foot orthosis powered by artificial pneumatic muscles," *J. Appl. Biomech.*, vol. 21, no. 2, pp. 189–197, 2005.

[38] J. A. Blaya and H. Herr, "Adaptive control of a variable-impedance ankle-foot orthosis to assist drop-foot gait," *IEEE Trans. Neural Syst. Rehabil. Eng.*, vol. 12, no. 1, pp. 24–31, Mar. 2004.

[39] M. Cestari *et al.*, "An adjustable compliant joint for lower-limb exoskeletons," *IEEE/ASME Trans. Mechatronics*, vol. 20, no. 2, pp. 889–898, Apr. 2015.

[40] S. Yamamoto *et al.*, "Comparative study of mechanical characteristics of plastic AFOs," *J. Prosthetics Orthotics*, vol. 5, no. 2, p. 59, 1993.

[41] M. D. J. J. Bregman *et al.*, "Polypropylene ankle foot orthoses to overcome drop-foot gait in central neurological patients: A mechanical and functional evaluation," *Prosthetics Orthotics Int.*, vol. 34, no. 3, pp. 293–304, 2010.

[42] S. Yamamoto *et al.*, "Development of a new ankle-foot orthosis with dorsiflexion assist, Part 1: Desirable characteristics of ankle-foot orthoses for hemiplegic patients," *J. Prosthetics Orthotics*, vol. 9, no. 4, pp. 174–179, 1997.

[43] J. Romkes and R. Brunner, "Comparison of a dynamic and a hinged ankle–foot orthosis by gait analysis in patients with hemiplegic cerebral palsy," *Gait Posture*, vol. 15, no. 1, pp. 18–24, 2002.

[44] S. Fatone *et al.*, "Effect of ankle-foot orthosis alignment and foot-plate length on the gait of adults with poststroke hemiplegia," *Arch. Phys. Med. Rehabil.*, vol. 90, no. 5, pp. 810–818, 2009.

[45] S. Miyazaki *et al.*, "Effect of ankle-foot orthosis on active ankle moment in patients with hemiparesis," *Med. Biol. Eng. Comput.*, vol. 35, no. 4, pp. 381–385, 1997.

[46] S. Yamamoto *et al.*, "Effects of plantar flexion resistive moment generated by an ankle-foot orthosis with an oil damper on the gait of stroke patients: A pilot study," *Prosthetics Orthotics Int.*, vol. 37, no. 3, pp. 212–221, 2013.
[47] N. B. Bolus *et al.*, "A novel method to assess angle sensor performance for wearable exoskeletal joint kinematics," in *Proc. 38th Annu. Int. Conf. IEEE Eng. Med. Biol. Soc.*, 2016, pp. 3109–3112.
[48] D. Bregman *et al.*, "A new method for evaluating ankle foot orthosis characteristics: BRUCE," *Gait Posture*, vol. 30, no. 2, pp. 144–149, 2009.
[49] J. Perry and J. M. Burnfield, "Gait analysis: Normal and pathological function," *J. Sports Sci. Med.*, vol. 9, 1992, Art. no. 353.
[50] S. H. Collins *et al.*, "Reducing the energy cost of human walking using an unpowered exoskeleton," *Nature*, vol. 522, no. 7555, pp. 212–215, 2015.
[51] T. Morita and S. Sugano, "Design and development of a new robot joint using a mechanical impedance adjuster," in *Proc. IEEE Int. Conf. Robot. Autom.*, 1995, vol. 3, pp. 2469–2475.

Nicholas B. Bolus (S'16) received the B.S. degree in mechanical engineering from the University of Alabama, Tuscaloosa, AL, USA, in 2015. He is currently working toward the Ph.D. degree in bioengineering with the Georgia Institute of Technology (Georgia Tech), Atlanta, GA, USA.

He serves as a Graduate Research Assistant in the laboratory of Dr. O. T. Inan with Georgia Tech. His research interests include the study of systems-level neuro-/biomechanics and the development of personalized, wearable devices for movement rehabilitation.

Mr. Bolus received the National Science Foundation Graduate Research Fellowship and the President's Fellowship at Georgia Tech.

Caitlin N. Teague (S'15) received the B.S. degree in electrical engineering, and the M.S. degree in electrical and computer engineering from the Georgia Institute of Technology (Georgia Tech), Atlanta, GA, USA, in 2014 and 2016, respectively, where she is currently working toward the Ph.D. degree with the Department of Electrical and Computer Engineering.

She is currently a Research Assistant in Dr. O. T. Inan's laboratory with Georgia Tech. Her research interests include the development of noninvasive biomedical devices and systems, particularly those that enable at-home long-term physiological monitoring.

Ms. Teague received the President's Fellowship from Georgia Tech in 2014.

Omer T. Inan (S'06–M'09–SM'15) received the B.S., M.S., and Ph.D. degrees in electrical engineering from Stanford University, Stanford, CA, USA, in 2004, 2005, and 2009, respectively.

He joined ALZA Corporation (A Johnson and Johnson Company), Mountain View, CA, in 2006, where he designed micropower circuits for iontophoretic drug delivery. In 2007, he joined Countryman Associates, Inc., Menlo Park, CA, where he was the Chief Engineer involved in designing and developing high-end professional audio circuits and systems. From 2009 to 2013, he was also a Visiting Scholar in the Department of Electrical Engineering, Stanford University. Since 2013, he has been an Assistant Professor of electrical and computer engineering with the Georgia Institute of Technology, Atlanta, GA, USA, where he is also an Adjunct Assistant Professor with the Wallace H. Coulter Department of Biomedical Engineering. He has authored or co-authored more than 100 technical articles in peer-reviewed international journals and conferences, and has multiple issued patents. His research focuses on noninvasive physiologic sensing and modulation for human health and performance, including for chronic disease management, acute musculoskeletal injury recovery, and pediatric care.

Dr. Inan is an Associate Editor of the IEEE JOURNAL OF BIOMEDICAL AND HEALTH INFORMATICS, an Associate Editor for the IEEE Engineering in Medicine and Biology Conference and the IEEE Biomedical and Health Informatics Conference, an Invited Member of the IEEE Technical Committee on Translational Engineering for Healthcare Innovation and the IEEE Technical Committee on Cardiopulmonary Systems, and a Technical Program Committee Member or Track Chair for several other major international biomedical engineering conferences. He received the Gerald J. Lieberman Fellowship in 2008–2009 for outstanding scholarship, the Lockheed Dean's Excellence in Teaching Award in 2016, and the Sigma Xi Young Faculty Award in 2017. He was a National Collegiate Athletic Association All-American in the discus throw for three consecutive years (2001–2003).

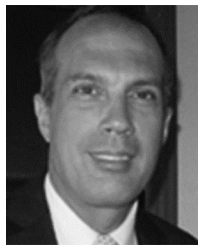

Géza F. Kogler was born in Detroit, MI, USA, in 1959. He received the B.F.A. degree in fine arts from Wayne State University, Detroit, in 1982; the post graduate certificate in orthotics from Northwestern University Prosthetics and Orthotics Center, Chicago, IL, USA, in 1983; and the Ph.D. degree in bioengineering from the University of Strathclyde, Glasgow, U.K., in 1998.

After working in clinical practices for several years, he joined the Orthotics Prosthetics Department, Florida International University, Miami, FL, USA, as an Instructor (1986–1991). He then took a position as the Instructor of clinical surgery at the Southern Illinois University School of Medicine, Springfield, IL, where he became an Assistant Professor in 1995 and an Associate Professor in 2001. He was a Visiting Associate Professor in the Department of Rehabilitation, Jönköping University, Jönköping, Sweden, in 2003. He was in clinical practice at Springfield Clinic, Springfield, (2003–2007) before joining the School of Applied Physiology, Georgia Institute of Technology, Atlanta, GA, USA, as a Research Scientist in 2008. He is currently the Program Director of the Master of Science in Prosthetic and Orthotics and Principal Investigator for the Clinical Biomechanics Laboratory, Georgia Institute of Technology. His current research interests include powered exoskeletal systems for rehabilitation, sensing applications for diagnostics and musculoskeletal health, foot–ankle biomechanics, and plantar foot tissue mechanics.

Dr. Kogler has received numerous awards for his research in foot–ankle biomechanics from the American Society of Biomechanics, the International Society of Biomechanics, and the International Society of Prosthetics and Orthotics, all of which he is an active member.